ON SELF ADAPTIVE RUNGE-KUTTA SCHEMES WITH IMPROVED ENERGY-CONSERVATION PROPERTIES

J. Plana-Riu, F.X. Trias, C.D. Pérez-Segarra, A. Oliva

Heat and Mass Transfer Technological Centre, Technical University of Catalonia, ESEIAAT. Carrer de Colom 11, 08222 Terrassa (Barcelona), Spain.

josep.plana.riu@upc.edu

Abstract

In this paper a novel approach to the computation of the eigenbounds of the system of ordinary differential equations is presented. Afterwards, this approach is applied for different Runge-Kutta methods with various properties among which the energy conservation in time is considered. By doing so, the energy budgets of these schemes applied to an inviscid flow as well as a three-dimensional Taylor-Green vortex.

1 Introduction

The numerical solution of any transport phenomenon within the Finite Volume Method (FVM) framework requires both space and time discretization of the governing equations. The incompressible Navier-Stokes equations (NS), which model the transport of mass, momentum and energy in a fluid, are no exception. In order to deal with this, the usual methodology starts by discretizing the equations in space, yielding the semi-discrete set of equations, using the notation from Trias, Lehmkuhl, et al. (2014),

$$M\mathbf{u}_s = \mathbf{0}_c, \quad (1a)$$

$$\Omega\frac{d\mathbf{u}_c}{dt} + C(\mathbf{u}_s)\mathbf{u}_c - D\mathbf{u}_c + \Omega G_c\mathbf{p}_c = \mathbf{0}_c, \quad (1b)$$

where M is the face-to-cell divergence operator, Ω_c is a diagonal matrix containing the cell volumes so that $\Omega = I_3 \otimes \Omega_c$, C_c is the cell-to-cell convective operator so that $C = I_3 \otimes C_c$, D_c is the cell-to-cell diffusive operator so that $D = I_3 \otimes D_c$, G_c is the cell-to-cell gradient operator, $\mathbf{u}_s$ is the velocity field defined at the faces, and I_3 is the identity matrix of size 3.

In order to integrate in time these equations, however, multiple techniques have been used during the development of the Computational Fluid Dynamics (CFD) theory. Pioneer studies from Parviz Moin and Kim (1982) used different integrating schemes for both convective, a second-order Adams-Bashforth (AB2) scheme; and diffusive, an implicit Crank-Nicholson; terms, while the sutides that followed generally used the projection method from Chorin (1968), integrating completely in time using an AB2.

Later studies from Kravchenko and Moin (1997) incorporated the use of second- ad third-order Runge-Kutta schemes (RK2, RK3) due to larger stability regions that provide larger timesteps. However, a general derivation for the use of these schemes was not published until Sanderse and Koren (2012).

Originally, most of the publications set timesteps according to the classical CFL condition from Courant, Friedrichs, and Lewy (1927), which provides a simpler approximation to the stability region of the simulation. Nonetheless, later on Trias and Lehmkuhl (2011) considered a free-parameter multistep time integrator $\kappa 1L2$ with an adaptable stability region, with an adaptive stability region due to the free parameter κ. This allowed an optimization of the simulation performance due to an increase on the timestep while keeping the simulation stable.

With regards to energy conservation, the influence of the space discretization has been widely studied in both structured (Verstappen and Veldman (2003)) and unstructured (Trias, Lehmkuhl, et al. (2014)) meshes, and it has been considered to be the most relevant, yet the influece of the time discretization in the kinetic energy budget of the simulation is much less studied. Originally, Sanderse (2013) proposed a set of symplectic RK schemes, yet its implicit nature leads to an additional computational cost that may preclude its application for large-scale simulations. In order to deal with that, Capuano, Coppola, and Luca (2015) developed and tested different pseudo-symplectic RK schemes in flow simulations, which are more efficient given their explicit construction.

2 Self-adaptive Runge-Kutta integration of the Navier-Stokes equations

Starting from the semi-discrete Navier-Stokes equations, Sanderse and Koren (2012) proposed the method for the integration with RK. Following its notation, an s-stage explicit RK can be applied to the integration of the NS equations as follows, note that the c subscripts have been dropped for simplicity reasons.

Rearranging the semi-discrete equations and defining

$F(\mathbf{u}_s)\mathbf{u}_c = \Omega^{-1}(D\mathbf{u}_c - C(\mathbf{u}_s)\mathbf{u}_c)$, and applying

the continuity equation, it can be derived that

$$\frac{d\mathbf{u}_c}{dt} = (I_n - GL^{-1}M)F(\mathbf{u}_s)\mathbf{u}_c, \tag{2}$$

where $I_n - GL^{-1}M$ is the so-called projection operator P, which leads to

$$\frac{d\mathbf{u}_c}{dt} = \tilde{F}(\mathbf{u}_s)\mathbf{u}_c, \tag{3}$$

being $\tilde{F}(\mathbf{u}_s) = PF(\mathbf{u}_s)$. In this system of ODE, however, the direct application of a Runge-Kutta scheme would be rather difficult since the construction of P would be complex. Hence, the projection method from Chorin (1968) can be applied, dividing this projection process in two different steps and thus not having to construct the operator.

Hence, with this splitting, for the inner stages, the method reads as follows,

$$\mathbf{u}_i^* = \mathbf{u}_n + \Delta t \sum_{j=1}^{i-1} a_{ij}\mathbf{F}_j, \tag{4a}$$

$$L\Psi_i = \frac{1}{c_i \Delta t} M\mathbf{u}_i^*, \tag{4b}$$

$$\mathbf{u}_i = \mathbf{u}_i^* - \Delta t G\Psi_i, \;\; i = 1, \ldots, s \tag{4c}$$

while for the last stage, it is slightly changed to

$$\mathbf{u}^* = \mathbf{u}_n + \Delta t \sum_{i=1}^{s} b_i\mathbf{F}_i, \tag{5a}$$

$$L\Psi_{n+1} = \frac{1}{\Delta t} M\mathbf{u}^*, \tag{5b}$$

$$\mathbf{u}_{n+1} = \mathbf{u}^* - \Delta t G\Psi_{n+1}, \tag{5c}$$

where b_i and a_{ij} are the scheme coefficients usually arranged in the so-called Butcher tableau (Butcher (2016)), $\mathbf{u}^*$ are the predictor velocities from Chorin's projection method, and Ψ are the first-order approximations to the pressure field. The time-step Δt will be set by making use of a self-adaptive algorithm.

Note that, in general, the initial velocity field might be incompressible analytically yet numerically those vectors do not fulfill $M\mathbf{u}_s = \mathbf{0}_c$. Hence, the field should be projected to the incompressible set of solutions. Let $\mathbf{u}_{0,a}$ be the initial field consisiting of the analytical function now discretized, hence, this would generate an initial pressure field $\mathbf{p}_0$ such that

$$L\mathbf{p}_0 = \frac{1}{\Delta t} M\mathbf{u}_{0,a}, \tag{6}$$

leading to the projection stage,

$$\mathbf{u}_0 = \mathbf{u}_{0,a} - \Delta t G\mathbf{p}_0 \tag{7}$$

In order to do so, the original method developed by Trias and Lehmkuhl (2011) will be replaced by a novel method since the original requires an explicit reconstruction in every iteration of both convective and diffusive matrices and thus more efficient methodologies are seeked.

Starting from a general semi-discretized scalar transport equation,

$$\frac{d\phi_c}{dt} + C_c(\mathbf{u}_s)\phi_c - D_c(\alpha_s)\phi_c = \mathbf{0}_c, \tag{8}$$

where ϕ_c is the transported scalar in the cells and α_s is the diffusivity at the faces; this revision the construction of the matrces has the following outcome, if a symmetr-preserving (SP) discretization is applied.

$$D_c(\alpha_s) = -T_{sc}A_s\Lambda_s\Delta_s^{-1}T_{cs} = -T_{sc}\tilde{\Lambda}_s T_{cs}, \tag{9a}$$

$$C_c(\mathbf{u}_s) = T_{sc}A_sU_s\Pi_{c\to s} \underbrace{=}_{SP} \frac{1}{2}A_sU_s|T_{cs}|, \tag{9b}$$

where T_{sc} is the face-to-cell incidence matrix, A_s is the face-to-face diagonal matrix containing the face diffusivities, $\Delta_s = \Omega_s A_s^{-1}$ is the diagonal matrix containing the projected distances between the centers of the cells adjacent to a given face f, $T_{cs} = T_{cs}^T$ is the cell-to-face incidenxe matrix, $\Pi_{c\to s}$ is the intepolator from cells to faces, and $U_s = diag(\mathbf{u}_s)$ is the diagonal matrix containing the vector field at the faces. This construction will hence allow computing the eigenbounds without the need of an explicit construction of the matrices. By doing so, a family of methods to compute the eigenvalues arise, with the parameter α arising from the theorem that states that, given a matrix $A \in \mathbb{R}^{n\times m}$ and a matrix $B \in \mathbb{R}^{m\times n}$, the matrices AB and A^TB^T will have the same eigenvalues except for the zero-values ones and thus, the following identity holds

$$\rho(D_c) = \rho(-T_{sc}\tilde{\Lambda}_s T_{cs}) = \rho(-\tilde{\Lambda}^\alpha T_{cs}T_{cs}^T\tilde{\Lambda}^{1-\alpha}), \tag{10}$$

where $\rho(\xi)$ is the spectral radius of the matrix ξ. For the convection matrix, in order to avoid reconstructing the matrix every iteration, it can be proven that

$$4\rho(C_c(\mathbf{u}_s)) \leq \rho(|F_s|^\alpha |T_{cs}T_{cs}^T||F_s|^{1-\alpha}). \tag{11}$$

Given that if the convective operator is skew-symmetric will have its eigenvalues located in the imaginary axis, and a symmetric diffusive operator will have them located in the real axis, it can be stated that the eigenvalues of the operator $\mathbf{F}_j$ will be bounded by

$$\lambda_F \leq -|\rho(D_c)| + i\rho(C_c(\mathbf{u}_s)). \tag{12}$$

For any given explicit Runge-Kutta scheme, its stability region (Fig. 1) can be determined by the general formulation from Butcher (2016)

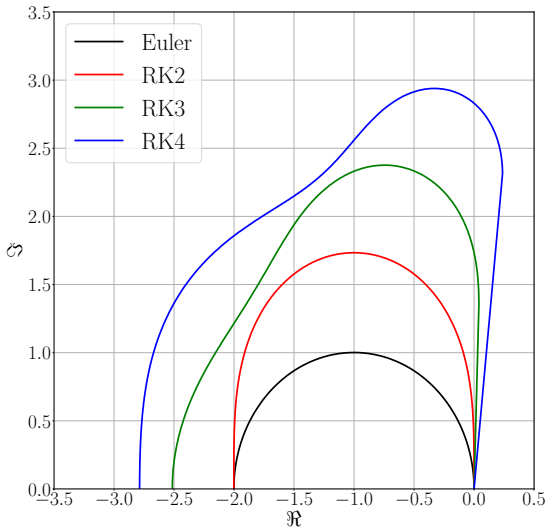

Figure 1: Stability region of different Runge-Kutta schemes.

$$R(z) = 1 + zb^T(I_s - zA)^{-1}\mathbf{1}, \tag{13}$$

where A is the matrix containing the a_{ij} coefficients of the Butcher tableau, as well as $b = (b_1\ b_2\ \dots\ b_s)^T$ and $\mathbf{1} = (1\ 1\ \dots\ 1)^T \in \mathbb{R}^s$, with $z \in \mathbb{C}$. Nonetheless, if the order of accuracy of the method coincides with the number of stages from the method (i.e. Euler, RK2, RK3, RK4), Eq. (13) can be rewritten as

$$R(z) = 1 + \sum_{p=1}^{s} \frac{1}{p!} z^p, \tag{14}$$

which simplifies notably the computation of the stability region for the method.

Hence, given the eigenbounds for the method as well as the stability region of the Runge-Kutta scheme, the maximum stable time-step Δt_{stab} will be computed following the methodology from Trias and Lehmkuhl (2011) by adding a scaling factor $f_{\Delta t}$ so that

$$\Delta t = f_{\Delta t} \Delta t_{stab}, \tag{15}$$

This allows checking the effect of $f_{\Delta t}$ on the energy budget of a simulation, as it is expected to lower the dissipation caused by the time integrating schemes-

3 Kinetic energy budget for the Navier-Stokes equations

In order to obtain a physics-compatible solver, the conservation of energy should be aimed. As it has been widely studied previously, the contributions in the energy conservation of the space discretization are strictly dependant on the construction of both convective and diffusive operators. By defining a global kinetic energy as $E = \mathbf{u}_c^T \mathbf{u}_c / 2 \in \mathbb{R}$, the semi-discrete kinetic energy equation reads as follows,

$$\mathbf{u}_c^T \Omega \frac{d\mathbf{u}_c}{dt} = -\mathbf{u}_c^T C(\mathbf{u}_s)\mathbf{u}_c - \mathbf{u}_c^T G_c \mathbf{p}_c + \mathbf{u}_c^T D \mathbf{u}_c. \tag{16}$$

Note that if the operators preserve their symmetries, i.e. D is symmetric, $C(\mathbf{u}_s)$ is skew-symmetric, and $G_c^T = -M$, the convective term contribution should vanish in every geometry (Trias, Lehmkuhl, et al. (2014)), while the pressure contribution will vanish in staggered configurations, so that the only contribution in energy variation, in the semi-discrete formulation, would be due to the diffusive term. Nonetheless, their contribution in the kinetic energy budget will be considered to verify the expected results.

When Eq. (16) is integrated in time, an additional term due to the energy imbalances from the time-integration appears,

$$\frac{\Delta E}{\Delta t} = E_{t,C} + E_{t,D} + E_{t,p} + \varepsilon_{RK}, \tag{17}$$

where $E_{t,C} = -\sum_{i=1}^{s} b_i \mathbf{u}_{c,i}^T C \mathbf{u}_{c,i}$ is the contribution from the convective term, $E_{t,D} = \sum_{i=1}^{s} b_i \mathbf{u}_{c,i}^T D \mathbf{u}_{c,i}$ from the diffusive term, $E_{t,p} = -\sum_{i=1}^{s} b_i \mathbf{u}_{c,i}^T G_c \mathbf{p}_{c,i}$ from the pressure gradient,

$$\frac{\Delta E}{\Delta t} = \frac{\mathbf{u}_c^{T,n} \Omega_c \mathbf{u}_c^n - \mathbf{u}_c^{T,n-1} \Omega_c \mathbf{u}_c^{n-1}}{\Delta t},$$

and ε_{RK} is the contribution from the Runge-Kutta scheme. As previously stated, it is expected that $E_{t,C} = E_{t,p} = 0$ in a staggered formulation, while a mathematical expression for ε_{RK} was proposed by Capuano, Coppola, and Luca (2015).

Nonetheless, this expression would be rather difficult to evaluate since it requires the use of the projection operator P and thus it is easier to evaluate it by difference with the other terms, which can be easily computed from the simulation results.

4 Numerical experiments

The numerical experiments carried out to validate the method will be split into two different categories. First of all, for a given time-step, an inviscid flow simulation has been performed in order to check that there was no energy dissipation due to the convective term as well as the pressure term, since their symmetry-preserving construction should lead to conservation with the same accuracy as the pressure solver. This problem will be solved making use of five different schemes (Tab. 1) so that their properties can be compared. These schemes will be the classical one-, two-, three- and four-stages Runge-Kutta schemes, as well as a six-stages pseudo-symplectic Runge-Kutta scheme first presented by Capuano, Coppola, and Luca (2015), named in their paper 4p7q(6), having fourth-order in accuracy and seventh in pseudo-symplecticity.

Table 1: List of the Runge-Kutta schemes used.

Method	Num. stages, s	Ord. accuracy, p
Euler	1	1
Heun RK2	2	2
Heun RK3	3	3
Standard RK4	4	4
4p7q(6)	6	4

Afterwards, the same Runge-Kutta schemes have been tested in a three-dimensional Taylor-Green vortex problem which will ensure that all components are well resolved.

This inviscid flow will be computed up to $t = 3$ s, in a cubic domain with side length 1.0 and will be started with a random distribution of values centered around 1.0 with a maximum value of 2.0 and a minimum value of 0.0, and then this field is turned incompressible by computing a pressure field and then projecting the velocity field to the incompressible space. Having a random flow will ensure that no error cancellation is observed. In order to test the method, it will be tested with a 64^3 mesh, with $\Delta t \in [10^{-4}, 5\times10^{-3}]$.

Note that, since the space discretization used in all the listed schemes in Tab. 1 is the same, the yield for the tests for the operators,

$$\mathbf{u}_c^T D\mathbf{v}_c - \mathbf{v}_c^T D\mathbf{u}_c = 0, \tag{18a}$$

$$\mathbf{u}_c^T C\mathbf{v}_c + \mathbf{v}_c^T C\mathbf{u}_c = 0, \tag{18b}$$

$$\max(M\mathbf{u}_s) = 0, \tag{18c}$$

where $\mathbf{u}_c, \mathbf{v}_c$ are vectors satisfying the incompressibility condition so that the skew-symmetry condition can be fulfilled, should be rather similar for all of them with any scheme (Fig. 2). Even though the figure just shows two different schemes, the similarity trend has been observed for every method used.

With regards to the energy budgets, it is expected that given the spectroconsistent discretization, both pressure and convective contributions to the energy variation should be zero (Fig. 3) in a structured and staggered setup as used. This has been observed in all the values of Δt used as well as for all the solvers from Tab. 1, yet for the sake of readibility, only three have been shown.

In regards to the three-dimensional Taylor-Green vortex, it has been initialized in a $2\pi\times2\pi\times2\pi$ domain, with the velocity field

$$u_{x,0} = U_0 \frac{2}{\sqrt{3}} \sin x \cos y \cos y \tag{19a}$$

$$u_{y,0} = U_0 \frac{2}{\sqrt{3}} \cos x \sin y \cos y \tag{19b}$$

$$u_{z,0} = U_0 \frac{2}{\sqrt{3}} \cos x \cos y \sin y \tag{19c}$$

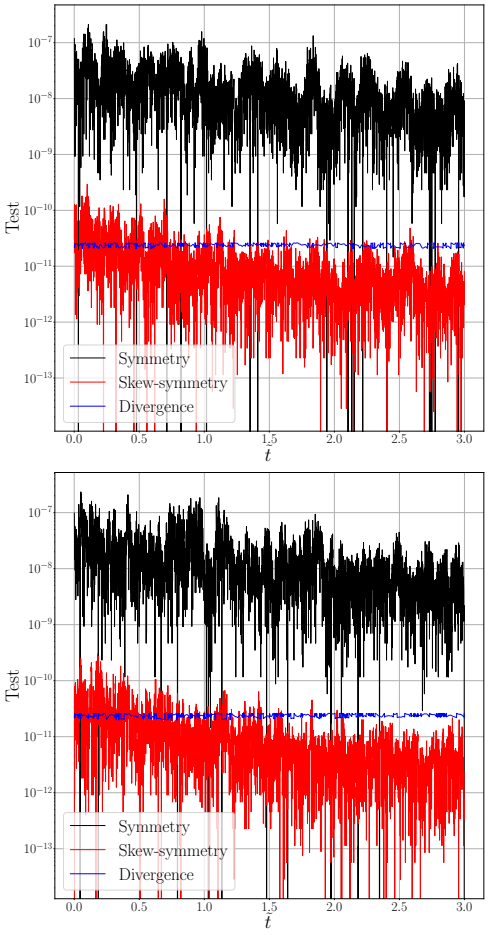

Figure 2: Yield of the symmetry-preserving spatial discretization tests for two of the solvers used for a given Δt. (Top) Heun RK2, $\Delta t = 10^{-4}$. (Bottom) 4p7q(6), $\Delta t = 10^{-4}$.

and run up until $\tilde{t} = 20$, being $\tilde{t} = t/(2\pi/U_0)$, as Capuano, Coppola, and Luca (2015). This has been run for two different Reynolds numbers, $\mathrm{Re} = [300, 3000]$, so that the effect of the Reynolds number can also be analyzed, with a mesh of 32^3 control volumes, and $f_{\Delta t} = \{0.1, 0.2\}$. Note that the different cases that are presented will have different time-steps, as their stability regions grow with the number of stages. With regards to the energy budgets, a notable change is obtained with the increase of Δt for all the used schemes (i.e. 4p7q(6) in Fig. 4) and thus the preservation of the energy (apart from the dissipation due to the time integrating scheme) will be reduced with bigger time-steps.

5 Conclusion

In this paper a novel method to compute the eigenbounds of the semi-discrete Navier-Stokes equations has been presented. With this method being applied, then different Runge-Kutta schemes with different properties concerning their energy preservation in time have been tested and their emergy budgets

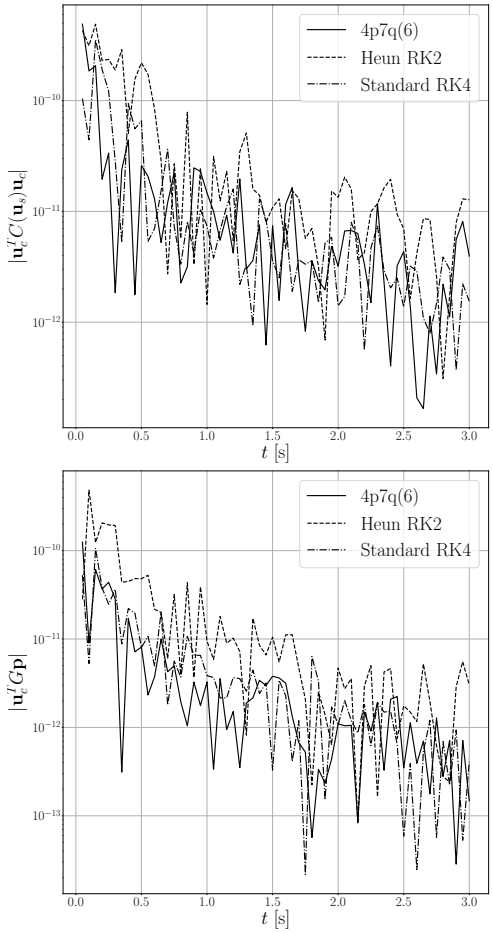

Figure 3: Energy budget contribution from the convective (top) and pressure (bottom) terms in the random inviscid flow simulations for $\Delta t = 5 \times 10^{-3}$.

for an incompressible three-dimensional Taylor-Green vortex problem have been presented.

Acknowledgments

The investigations presented in this paper are supported by the *Ministerio de Economía y Competitividad*, Spain, RETOtwin project (PDC2021-120970-I00). J.P-R. is also supported by the Catalan Agency for Management of University and Research Grants (AGAUR). The authors thankfully acknowledge these institutions.

References

Butcher, J. C. (2016). *Numerical Methods for Ordinary Differential Equations*. Wiley. ISBN: 9781119121503.

Capuano, F., G. Coppola, and L. de Luca (2015). "An efficient time advancing strategy for energy-preserving simulations". In: *Journal of Computational Physics* 295, pp. 209–229.

Chorin, Alexandre Joel (1968). "Numerical Solution of the Navier-Stokes Equations". In: *Mathematics of Computation* 22(104), pp. 745–762.

Courant, Richard, Kurt Friedrichs, and Hans Lewy (1927). "Über die partiellen Differenzengleichungen der mathematischen Physik". In: *Mathematische Annalen* 100(1), pp. 32–74.

Kravchenko, A G and P Moin (1997). "On the Effect of Numerical Errors in Large Eddy Simulations of Turbulent Flows". In: *Journal of Computational Physics* 131, pp. 310–322.

Moin, Parviz and John Kim (1982). "Numerical investigation of turbulent channel flow". In: *Journal of Fluid Mechanics* 118, pp. 341–377.

Sanderse, B. (2013). "Energy-conserving Runge-Kutta methods for the incompressible Navier-Stokes equations". In: *Journal of Computational Physics* 233(1), pp. 100–131.

Sanderse, B. and B. Koren (2012). "Accuracy analysis of explicit Runge-Kutta methods applied to the incompressible Navier-Stokes equations". In: *Journal of Computational Physics* 231(8), pp. 3041–3063.

Trias, F. X. and O. Lehmkuhl (2011). "A self-adaptive strategy for the time integration of Navier-Stokes equations". In: *Numerical Heat Transfer, Part B: Fundamentals* 60(2), pp. 116–134.

Trias, F. X., O. Lehmkuhl, et al. (2014). "Symmetry-preserving discretization of Navier-Stokes equations on collocated unstructured grids". In: *Journal of Computational Physics* 258, pp. 246–267.

Verstappen, R. W.C.P. and A. E.P. Veldman (2003). "Symmetry-preserving discretization of turbulent flow". In: *Journal of Computational Physics* 187(1), pp. 343–368.

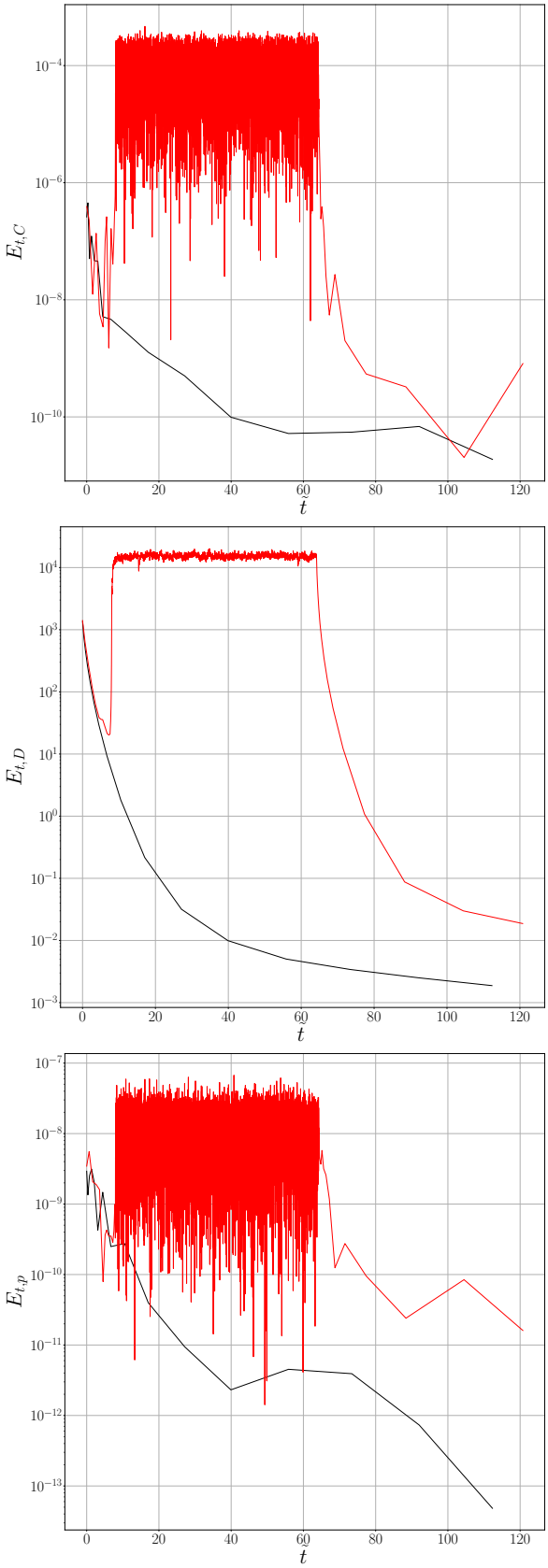

Figure 4: Energy budgets for a Re=3000 Taylor-Green vortex run for two different $f_{\triangle t} = \{0.1, 0.2\}$ with a 4p7q(6) pseudo-symplectic Runge-Kutta scheme.